Effect of Fin Configuration on the Performance of Longitudinal Fin Arrays

تأثير شكل الزعنفة على أداء مصفوفات ذات زعانف طولية

E. A. M. Elshafei, E. A. El-Negiry
Mechanical Power Eng. Dept., Mansoura Univ., Mansoura, Egypt
Eellshafei@mans.edu.eg, Emad-elngiry@yahoo.com

الخلاصة

يهدف هذا البحث إلى دراسة معملية لخصائص انتقال الحرارة والسريان خلال مصفوفات زعانف طولية بأشكال مختلفة معزولة أطرافها ومثبتة على قاعدة ساخنة تغذى بفيض حراري منتظم في مجرى هوائي حاكم لضمان مرور الهواء كاملا خلالها. تم بيان تأثير شكل الزعنفة على الأداء الحراري وفقد الضغط لثلاث مصفوفات ذات حجم وكثافة زعانف ثابتين. ولقد أجريت التجارب على ثلاث مصفوفات هي ذات الزعانف المستقيمة وذات الزعانف المتعرجة المتماثلة والثالثة خليط من الزعانف المستقيمة والمتعرجة مرتبة على التوالي. أخير أداء المصفوفات الثلاث عند معدلات تصرف هواء مختلفة حيث يتغير رقم رينولدز من ٢×١٠ ٤ إلى ٤,٦ × ١٠ ٤ تقريبا وقيم مختلفة للفيض الحراري المنتظم. أظهرت النتائج أن أداء المصفوفات لا يتأثر بتغير الفيض الحراري وأن معامل انتقال الحرارة بالحمل من المصفوفة مخلطة الزعانف إلى الهواء يزيد بمقدار ٦٨% تقريبا وأن فقد الضغط لوحدة الطول خلالها يزيد بمعامل قدره ٥,٦ تقريبا مقارنة بمصفوفة الزعانف المستقيمة. بينما يزيد معامل انتقال الحرارة بالحمل من مصفوفة الزعانف المتعرجة المتماثلة إلى الهواء حوالي ٣٠ % ومعامل فقد الضغط حوالي ٢,٦ مقارنة أيضا بمصفوفة الزعانف المستقيمة. وبمقارنة نتائج انتقال الحرارة لمصفوفة الزعانف المستقيمة بنتائج الأبحاث السابقة على مثيلتها وجد تطابق معقول في ظروف تشغيل متشابهة من حيث معدلات سريان الهواء ونسبة ارتفاع الزعنفة إلى المسافة البينية بين الزعانف.

Abstract

Heat and fluid flows characteristics for ducted longitudinal fin arrays with different fin configurations under forced air-cooling have been investigated experimentally. The fins are attached to a heated base plate, while their tips are insulated and fully shrouded to avoid leakage. The aim of the study is to investigate the effect of fin configuration on thermal performance of fin arrays and pressure drop across them. Tests are performed on all straight, all corrugated and mixed fin arrays. The Reynolds number is ranged from $2x10^4$ to $4.6x10^4$, while the fin density and heat sink volume are kept unvaried. For the heat transfer and pressure drop measurements, the mixed fin array offered the best heat transfer coefficient with the highest-pressure drop. Over the tested range of airflow rates, the enhancement of heat transfer coefficients for the corrugated and mixed fin arrays compared to that of the straight fin array are found to be about 30% and 68%, while the pressure drops per unit longitudinal length of the fin array increase by a factor of 2.6 and 5.6 respectively. The heat transfer results for the straight fin array fairly agreed with those reported in literature.

Keywords:, Fin array, Enhancement of heat transfer, Cooling of electronic equipment.

Nomenclature

A_t	total surface area of fin array, m^2	L_c	longitudinal length of fin array, m
A_F	free flow area, m^2	L_p	corrugation pitch, m
A_{fc}	fin cross section area, m^2	M	parameter, equation (6)
D_h	hydraulic diameter, m	m	parameter, equation (7)
f	coefficient of friction	N_f	number of fins
h	heat transfer coefficient, W/m^2 K	Nu	Nusselt number, (hD_h/k_a)
H	duct height, m	P	pressure, Pa
k	thermal conductivity, W/m K	Q	rate of heat transfer, W

Accepted June 3, 2003.

p perimeter, m
Pr Prandtl number, ($Cp\ \mu/k_a$)
Re Reynolds number, ($v_m\ D_h\ /\upsilon$)
S fin gap width, m
t_f fin thickness, m
T temperature, K
v air velocity, m/s
v_m maximum velocity through the fin array, m/s
w fin array width, m
Y pressure drop ratio, ($\Delta P/\ \Delta P_a$)

Greek Symbols

β corrugation angle
θ temperature rise, K
ν kinematic viscosity, m^2/s
ρ density. Kg/m^3

Subscripts

a air
av average
b brass, base, bulk air
fc fin cross-section
f fin
h hydraulic
min minimum
s straight
t total
L loss

1-Introduction

The increase in power density of electronic equipment is requiring more effective thermal enhancement to cool its components and to maintain its operating temperature at a satisfactory level. One of the most common and attractive ways is using forced air cooling through the use of extended surface heat sinks. That is due to its simplicity and cost effectiveness. However, the flow field surrounding the heat sink caused by fin geometry is very complicated. Design of such heat sink takes the form of longitudinal fin array affixed to a base plate. To avoid diminishing of the rate of heat transfer due to longitudinal flow leakage out of the interfin spaces into the ambient, the heat sink should be fully shrouded.

Experimental data collected from various studies presented in literature, utilized heat sinks with relatively thick fins and moderate fin spacing. The studies did not elaborate on the loss of airflow from the top of the heat sink and the distribution of airflow through the various regions of the duct. These fins are usually treated as a conduction problem while the convection and fluid mechanic processes within the adjacent flow to the fin and its base have not been much tackled. A constant heat transfer coefficient is assumed and introduced to the conduction analysis of the fin.

Laminar flow heat transfer analysis of fully and partially shrouded fin array was numerically investigated by Sparrow et al (1978). Numerical and experimental study of the performance of shrouded longitudinal fin arrays under forced convection was presented by Sparrow et al (1981), Kadle et al (1986) and Sparrow et al (1986). They reported that the lowest values of the heat transfer coefficients were at the fin base/plate intersections and at the fin/shroud intersections and their values from experimental data agreed with those for uniformly heated circular tube. It was reported (in Sparrow et al (1986)) also that the heat transfer rates diminished with the increase of shroud clearance relative to that of no-clearance case, and were independent of both the airflow rate and the used fin efficiency model in evaluating the heat transfer coefficient.

Recently, the design and performance of fin arrays heat sinks used in cooling of electronic equipment by forced convection have received more attention from researchers. Bejan et al (1992) has detected tbe optimal fin spacing for maximum heat transfer from a longitudinal fin array heat sink cooled by forced convection. In his study of the performance of heat sink, Metrol (1993) has determined its

dimensions by using thermal resistance according to heat dissipation and surrounding flow velocity. The effect of bypass flow over fins due to clearance between fins tips and duct wall has been taken into account. Wirtz (1994) studied the effect of bypass flow on longitudinal fin array performance and reported that the overall rate of heat transfer and the pressure drop across the fin array are reduced due to the increase of flow bypass factor. His results agreed with that of Sparrow et al (1986). Experimental results of Butterbaugh et al (1995) indicated the thermal resistance to correlate strongly with the pressure drop across the ducted heat sink, while appearing to be relatively independent of shroud clearance.

Adam et al (1997) investigated the performance and flow behavior of fully and partially shrouded fin array heat sinks with different geometry under forced air-cooling. In their study, they used a computational fluid dynamics code. They reported that tbe increased rate of heat transfer was mainly due to tbe increased surface area available for heat transfer to the fluid with dense fin array. However, as observed by Writz et al (1994), much of gain in the overall heat transfer rate is offset by reduction in heat transfer coefficient occurred due to the accompanied increase of flow bypass. Adam et al (1997) also noticed that tbe effect of flow bypass on local heat transfer coefficient diminished beyond a certain shroud clearance as well as along the fin array. The latter notice was related to the boundary layer development from the entrance towards the exit. Regarding pressure drop across fin arrays, Adam et al (1997) observed that its magnitude increased with fin density and decreased with the increase of both Reynolds number and flow bypass. They related the discrepancy in friction factor compared with that of flat plate to the undeveloped flow across the fin arrays heat sinks.

Suzana et al (2000) studied the performance of a ducted rectangular plate fin heat sink. They reported that the thermal resistance decreased with the increase of both flow rate and fin density and independent of heat input. However, the pressure drop increased and became more pronounced with high mass flow rate. Their experimental results, numerical results using CFD code and analytical predictions based on Holman et al (1996) model have the same trend and few discrepancies between them have been noticed. In-line and staggered parallel-plate fin arrays were investigated, both numerically and experimentally, by Sathyamurthy et al (1996). It was found that the thermal performance of the staggered fin configuration was better than that of the planer fin configuration over the power and flow ranges examined. The enhanced thermal performance however, was realized at the expense of an additional pressure drop. The effects of geometry of parallel-plate fin heat exchangers were also investigated by Zhang et al (1997).

The fin geometry effects on the heat transfer and flow behavior are investigated on interrupted fin surfaces by Hatada et al (1984), Webb et al (1990) and DeJong et al (1999). These interrupted surfaces consisted of flat plates either aligned with the main flow or at an angle of attack as in louvered-fin designs, and convex-louvered fin arrays. They reported that the improvement in thermal performance over that of continuous fins is due to the restart of thermal boundary layer and its thinning as well as the mixing and unsteadiness flow promoted at some critical Reynolds number.

Although results for fully and partially shrouded straight fin arrays as well as interrupted louvers and convex-louver geometries over a range of fin pitches and Reynolds numbers have been reported in the literature, Little work has been directed at the continuous corrugated and mixed fin geometries. The aim of the present work is to investigate the performance of fully shrouded longitudinal arrays which have

different fin geometries. These arrays works under forced air cooling where Reynolds number ranges from $2x10^4$ up to $4.6x10^4$.

2- Experimental Setup

2.1.Test Loop

The open loop wind tunnel with its main components used in experiments is depicted in Fig. 1. It is provided with a flow control gate , blower, the test section, the power supply, temperature and flow measurements devices. The entrance section of the tunnel of a rectangular cross section preceding the test section was made of wood and long enough to assure undisturbed and fully developed flow upstream of the test section.

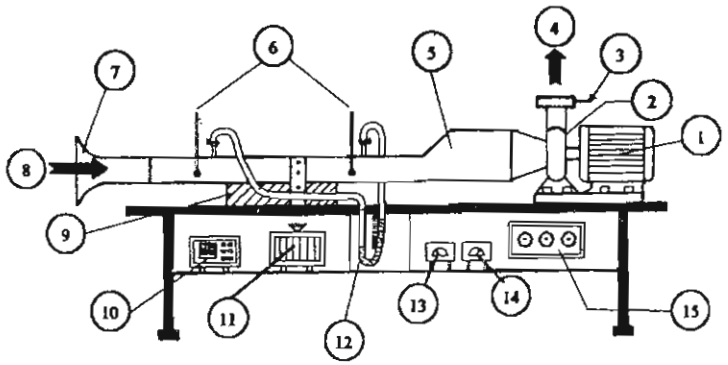

Fig.1. Test Rig

1- Electric motor, 2- Suction air blower, 3- Air flow control gate, 4- Air stream out, 5- Wooden duct, 6- Temperature probes, 7- Bell mouth, 8- Air in, 9- Test section, 10- Digital temperature recorder, 11-Autotransformer, 12- Manometer, 13- Voltmeter 14- Ammeter 15, Blower operating switchboard.

2-2. The Test Section

The test section dimensions of 107 x225x51 mm allow to accommodate the three different geometries of fin arrays. Its details are shown in Fig.2. As can be seen, it mainly consists of fin array, a heated base plate and a wooden shroud. The entire array can be mounted in that test section in the wind tunnel to facilitate good thermal contact between its surface and the heating source, and to expose the fins to a nearly uniform air flow having a variable velocity ranged from 1.5 up to 30 m/s.

The fins are made of brass because of easy machinability and welding processes to the upper face of the fin base plate which is also made of brass and has an external dimensions of 3 x 107x 225 mm. An electrical resistance wire, which provides heat to the fin array, is sandwiched by two mica sheets and placed in contact with the base plate of the fin array heat sink and fitted into a wooden box containing a block of Styrofoam. With the exception of the block, which is in contact with the fin array, the heat unit is completely insulated on all sides. This insulation is assumed to direct all heat transfer into the fin array.

The closure of the fin gaps flow passages of the heat sink is accomplished by the U-shaped cross section wooden shroud, which is attached to the fin base plate at its

outboard edges and sealed as well with the top edges of the fin array. This helped to minimize heat losses by conduction from the base plate through the shroud and prevent air leakage.

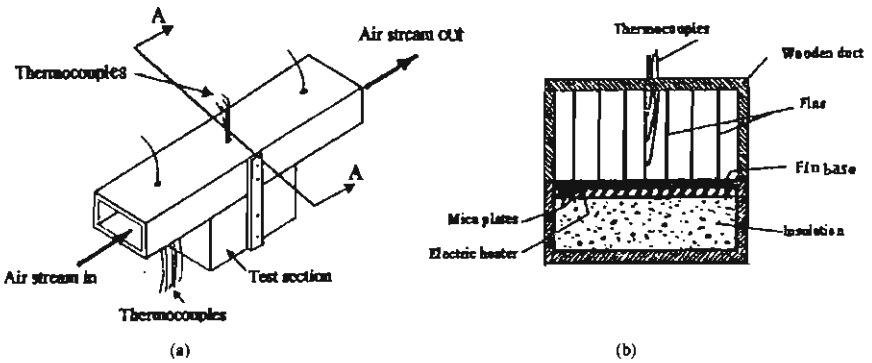

Fig. 2. Test Section, (a) view of test section, (b) cross sectional view at AA

As can be noticed in Fig. 2, there are a total of 7 fins. The shroud-adjacent side passages are half as wide as the interior passages.

The wind tunnel is run in suction mode. Air is drawn from the laboratory through its developing entrance length, then passed a calibrated velocity meter into the test section. From there, the air is sucked through a rectangular duct by a centrifugal fan followed by a graduated control airflow gate.

2-3. Heating Process and Instrumentation

The power is supplied to the heater by a regulated AC source via an autotransformer to control the voltage. The heater voltage drops and the current are measured by a multi-meter. The voltage settings for the heater are guided by the inserted thermocouples in the test section. Tests are carried out on three different fin arrays. The details of these arrays are shown in Fig. 3.

A 9 copper-constantan (type T) thermocouples are embedded into one-mm diameter 9 holes drilled in the bottom surface of the base plate.

Another 10 thermocouple probes are also positioned longitudinally along the surface of the central fin in the array and covering the distance from base to tip. 6 of them are inserted at half of its height and the rest at its tip. All thermocouple probes are assured to be in good contact with the fin and base-plate surfaces. To measure the temperature of inlet and outlet air, 4 thermocouples are inserted 100-mm up-stream of the test section, and another 4 thermocouple probes 60-mm downstream of it respectively. Temperatures are recorded by connecting thermocouples to a digital temperature recorder of 0.1°C resolution and with an accuracy of ± 0.5°C (model 3087).

The graduated gate at the wind tunnel exit controlled airflow rates. A calibrated hot wire anemometer and a traversing mechanism, 150-mm ahead of the test section measured the mean air velocity. The actual velocity of the air stream through the fin arrays is evaluated taking into account the blocked area due to the presence of fins. For all tested fin arrays, this blocked area is about 7% of that of the fin array cross sectional area.

Two static pressure taps are located up-stream and downstream of the test section to measure the pressure drop across the fin array by connecting them to a U-tube water manometer.

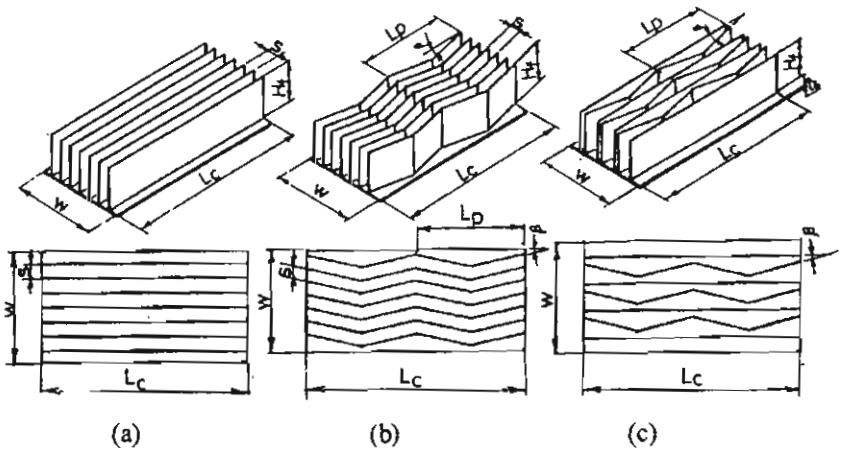

Fig. 3. Tested Fin Arrays Geometry and their Top Views, (a) Straight fin array, (b) Corrugated fin array, (c) Mixed fin array

3-Test Procedure and Data Reduction

3-1. Procedure

The dimensional values used in the study are summarized in Table 1. Each fin array is described in terms of its dimensions and corrugation angle β.

Table 1: Geometrical Parameters of Tested Fin Arrays.

Parameter	Range		
	Straight Fin Array	Corrugated Fin Array	Mixed Fin Array
A_t ; fin array surface area	0.183 m^2	0.188 m^2	0.185 m^2
A_t/A_{ts}, area ratio	1.0	1.07	1.03
N_f; number of fins	7	7	4 straight, 3
t_b ; base plate thickness	3 mm	3 mm	corrugated
t_f ; fin thickness	1 mm	1 mm	3 mm
L_c ; longitudinal length	225 mm	225 mm	1 mm
L_f ; fin length	L_c	$L_c/\cos\beta$	225 mm
L_p; corrugation pitch	-	$L_c/2$	L_c, $L_c/\cos\beta$
w; fin array width	107 mm	107 mm	$L_c/2$
H_f, fin height	51 mm	51 mm	107 mm
S; fin gap width	13 mm	13 mm	51 mm
β ; corrugation angle	0	14°	6mm-20mm
			14°

The investigation covers three fin arrays of 7 fins, all straight fin array, all corrugated fin array, and mixed (straight with corrugated) fin array. All arrays have equal volume and the total surface area of each of them is also calculated to be nearly equal. They are tested for three power inputs, 48 W, 100 W, and 150 W at different airflow rates in terms of Reynolds number.

During runs, a heat balance test for the heated base plate of the straight fin array with its environment at the maximum power input of 150 W was carried out. It was observed that the heat leakage rate from the outer surface of the fin base insulation assembly was about 1.5 W which represents 1% of the total power input, indicating that the heat leakage rate can be ignored.

Heat transfer and pressure drop results are parameterized by conventional rectangular duct Reynolds number based on the hydraulic diameter D_h, defined as

$$\mathrm{Re} = \frac{v_m D_h}{\nu} \tag{1}$$

Where v_m is the maximum velocity through the fin array and D_h is the hydraulic diameter, given by

$$D_h = \frac{4 A_F L_c}{A_s} \tag{2}$$

Where L_c is the core length of the fin array and A_F is the free flow area expressed as

$$A_F = (w - N_f t) H_f \tag{3}$$

For the straight fin array, A_t is given by:

$$A_t = L_c(2N_f H_f) + L_c(w - N_f t) \tag{4}$$

The total surface area of corrugated fins among the other two arrays is calculated using the above equation with longitudinal fin length of $L_c / \cos \beta$.

The fin array was installed in its position inside the test section. Adjusting the input voltage and the electric current via an auto-transformer controlled the input power to the base plate. To attain a steady state condition, the system was initially run for about one hour until constant values of the recorded temperatures of both the bulk air and the array surface at the points of measurements are observed.

3-2. Data Reduction

Air with uniform upstream velocity v and temperature t_b is flowing through the ducted fin array exchanging heat transfer with it. The test section was completely insulated so that heat transfer from fin array to ambient can be neglected. The rate of heat dissipated to air from the fin array by conduction as well as by forced convection can be described as

$$Q_f = M \tanh mH_f \tag{5}$$

Where,

$$M = \sqrt{hp_f k_f A_{fc}}\, \theta_b, \tag{6}$$

$$m = \sqrt{\frac{hp_f}{k_f A_{fc}}} \tag{7}$$

And θ_b is the excess temperature of the fin array base plate

The parameters M and m are related to each one of the tested fin arrays and Q_f described by equation (5) is also given by

$$Q_f = Q_{in} - Q_{fb} - Q_L \tag{8}$$

Where Q_{in} is the power input to the fin array, Q_{fb} is the rate of heat transferred by convection from the base plate area represented by gaps between the fins, defined as

$$Q_{fb} = hL_c(w - N_f t)\theta_b \tag{9}$$

and Q_L is the rate of heat loss which is being neglected. Substituting equations (5) and (9) with the parameters m and M into equation (8), then

$$Q_{in} = h\theta_b L_c(w - N_f t_f) + N_f \sqrt{hp_f k_f A_{fc}}\,\theta_b \tanh\sqrt{\frac{hp_f}{k_f A_{fc}}} H_f \tag{10}$$

Heat transfer results for the tested fin arrays are represented in terms of Nu, which is

$$Nu = \frac{h D_h}{k_a} \tag{11}$$

The ability of each of these fin arrays in transferring a given quantity of heat, where the fin temperature varies from its base-to tip is measured by fin efficiency. This term is defined as the ratio of the heat dissipated from the fin to the maximum heat transfer rate that would exist if its entire surface were at the base temperature. Considering one-dimensional heat flow (conduction model), the fin efficiency is

$$\eta_f = \frac{\tanh mH_f}{mH_f} \tag{12}$$

The values of heat transfer coefficient (h) are obtained by iteration from the experimental data using a simple computation program to solve equation (10). The iteration was continued until convergence, and then used as an input to equation (11) and (12).

Another quantity characterizing the flow across the fin array is the total pressure drop per unit longitudinal length of the fin array ($\Delta P / L_c$), which interpreted using the conventional definition

$$\Delta P / L_c = f \frac{\rho v_m^2}{2 D_h} \tag{13}$$

4. **Results and Discussion**

Average Nusselt Numbers, Figure 4 shows the variation of the average Nusselt number with Reynolds number for the straight fin array at 3-power inputs, 48 W, 100 W and 150 W. At constant power input, it is seen that Nu increases with Re. It is also noticed that a little change in heat transfer coefficient with varying power input, especially at high air mass flow rate. The latter notice agrees what has been reported by Suzana et al (2000). For the corrugated fin array, as shown in Fig. 5, the increase of Reynolds number has the same effect on heat transfer coefficient as in the straight fin array with negligible effect for power input variation. It is also noticed from Fig.6 that for the mixed fin array, the heat transfer coefficient is insensitive to the variation of power input and tremendously increases with the increase of Reynolds number.

Comparing the results for the three fin array configurations, it is seen from Fig. 7 that the mixed fin array has the highest heat transfer coefficients over the entire range of Reynolds number. That enhancement in heat transfer coefficients may be due to the higher flow velocity at sections of small area between the corrugated fins and the straight ones and because flow acceleration thins the boundary layer. The values of Nu number for the corrugated fin array are generally lie between those of straight and mixed fin arrays. It is also seen from Fig. 7, that the discrepancies between the values of Nu numbers for all arrays decrease with the increase of Reynolds number.

Figure 8 shows the percentage increase in Nusselt number due to fin configuration. It is observed that for $7000<Re<25000$, the increase in Nusselt number for corrugated and mixed fin arrays related to that of straight fin array is about 40% and 85% respectively. For $Re> 25000$ up to 47000, that increase is about 20% and 50% respectively. The reduction in enhancement of heat transfer coefficient at high Reynolds number may be attributed to the increase of flow unsteadiness due to flow separation through the passages of both mixed and corrugated fin arrays. The unsteadiness flow is more pronounced with the mixed fin array. As reported by DeJong et al (1999) based on flow visualization study, this flow unsteadiness begins at downstream locations and progressively moves upstream as the Reynolds number increases.

It is also noticed from Fig. 8 that with the increase of Reynolds number, the thermal performance of both corrugated and mixed fin arrays moves towards that of the straight fin array. This indicates that the effect of fin corrugation decreases with the increase of Reynolds number.

Fin Efficiency, The values of fin efficiency evaluated from equation (12) for the three-fin arrays are plotted in Fig. 9. For a specific fin array geometry, it is observed that the fin efficiency decreases with the increase of Reynolds number. This reflects the Reynolds number related increase in convective heat transfer coefficient and the domination of convection heat transfer mode rather than conduction one. The measured data showed that, at certain flow rate, the mixed fin array has the highest temperature gradient along the fin height. This results in a reduction in the rate of conducted heat transfer through the fins of that array. At constant Reynolds number, therefore the mixed fin array of highest heat transfer coefficients has the lowest fin efficiency, which is based on conduction model.

Pressure Drop, The pressure drop component ($\Delta P / L_c$) across the tested fin arrays as a function of Reynolds number is shown in Table 2 and plotted in Fig. 10.

Table 2. Pressure drop per unit core length as a function of *Re* for the three fin arrays.

		Straight Fin Array N_f=7, S=13 mm, L_c = 225 mm.	**Corrugated Fin Array** N_f =7, S=13 mm, β=14°,L_p = 112.5 mm	**Mixed Fin Array** N_f=7, S = 6-20 mm β=14°,L_p = 112.5 mm
v_m, (m/s)	$Re \times 10^{-3}$	$\Delta P/L_c$ (Pa/m)	$\Delta P/L_c$ (Pa/m)	$\Delta P/L_c$ (Pa/m)
1.6	2.5	5	9	15
4.8	7.5	34	45	65
10.2	16.0	98	283	530
17.7	27.8	280	818	1680
25.2	39.7	542	1267	2750
29.5	46.4	720	1510	3460

It is observed from Fig. 10 that the pressure drop increases dramatically for all three geometries with the increase of Reynolds number. The highest-pressure drops belong to the mixed fin array. This may be urged to the increased flow acceleration resulted from the change in flow cross section among that mixed fin array and the occurred flow separations. However, as can be seen in Fig. 11, the ratio ($Y = \Delta P/\Delta P_{st}$) of pressure drop across the corrugated and mixed fin arrays and that of the straight one decreases with the increase of Reynolds number and the performance of both corrugated and mixed fin arrays seems to move towards that of the straight one. This indicates that the effect of corrugation is expected to diminish at higher values of Reynolds numbers.

Comparison with Others, A comparison between the present heat transfer results of the straight fin array and the reported data from literature is shown in Fig. 12. It can be noticed that the present results are fairly close to that reported by Kadle and Sparrow (1986) over their tested range of Reynolds number (up to 30000) and show a slight difference for higher Reynolds number. The small discrepancies may be due to the differences in flow passage geometry. The results also have the same trend as those represented by Petukhov-Popov equation (in Holman, J. P., 1981) for fully developed turbulent flow in a uniformly heated circular tube for $Re \geq 10000$.

CONCLUSION

An experimental investigation has been carried out to investigate the effect of fin configuration and flow regimes on thermal performance of ducted fin arrays and pressure drop across them. The heat transfer coefficients for all three tested fin arrays are found to increase tremendously with increasing air velocity and invariant with power input. The parabolic dependence of the pressure drop across all fin arrays on air velocity is also seen. The mixed fin array offered the highest values of heat transfer coefficients accompanied with the highest-pressure drops. This may be attributed to the promoted vortices and flow separations. Over the tested air flow range, the percentage increase in Nu for both corrugated and mixed fin arrays related to that of the straight one is about 30% and 68% respectively, while the pressure drop ratio ($Y=\Delta P/\Delta P_{st}$) increases by a factor of about 2.6 and 5.6. Based on these results, the enhancement in thermal performance accompanied with fin corrugation at the

expense of pressure drop is dependent on Reynolds number. The effect of corrugation seems to diminish at higher values than the tested range of Reynolds number. Heat transfer results for the straight fin array fairly agree with those reported in literature.

References

- Adam, V. B., and Izundu, F.,O., "Characterization of Longitudinal Fin Heat Sink-Thermal Performance and Flow Bypass Effects Through CFD Method," Semitherm, Thermal and Fluid Flow Analysis Software, MAYA, 1997.
- Bejan, A., Sciubba, E., "The optimal Spacing of Parallel Plates Cooled by Forced Convection," Int.J. Heat & Mass Transfer, Vol.35, No.12, 1992, pp.3259-3264.
- Butterbaugh, M. A., and Kang, S. S., "Effect of Airflow Bypass on the Performance of Heat Sinks in Electronic Cooling," ASME Proceeding of Advances in Electronic Packaging, Vol.2, pp.843-848, 1995.
- DeJong, N. C., and Jacobi, A. M., "Local Flow and Heat Transfer Behavior in Convex-Louver Fin Arrays," ASME J. of Heat Transfer, Vol. 121, pp.136-141, 1999.
- Hatada, T., and Senshu, T., "Experimental Study on Heat Transfer Characteristics of Convex Louver fins for Air Conditioning Heat Exchangers," ASME Paper 84-HT—74, ASME, New York.
- Holman, J. P., "Heat Transfer, 5th ed., McGraw-Hill, New York, 1981.
- Kadle, D. S., Sparrow, E. M., "Numerical and Experimental Study of Turbulent Heat Transfer and Fluid Flow in Longitudinal Fin Arrays," ASME J. of Heat Transfer, Vol.108, pp.16-23, 1986.
- Metrol, A., "Optimization of Extruded Type External Heat Sink for Multi-chip Module", J. of Electronic Packaging, Vol.115, pp.440-444, 1993.
- Sathyamurthy, P., Runstodler, P. W., and Lee, S., "Numerical and Experimental Evaluation of Planner and Staggered Heat Sinks," Proceeding of the 5th Inter Socicty Conference on Thermal Phenomena in Electronic Packaging, pp. 132-139, 1996.
- Sparrow, E. M., Baliga, B. R., Patankar, S. V. " Forced Convection Heat Transfer from a Shrouded Fin Array with and without Tip Clearance," ASME J. of Heat Transfer, Vol. 100, pp.572-579, 1978.
- Sparrow, E. M., Beckley, T. J., "Pressure Drop Characteristics for a Shrouded Fin Array with Tip Clearance," ASME J. of Heat Transfer, Vol.103, PP.393-395, 1981.
- Sparrow, E. M., Kadle, D. S., "Effect of Tip-to-Shroud Clearance on Turbulent Heat Transfer From a Shrouded, Longitudinal Fin Array," ASME J. of Heat Transfer, Vol.108, pp.519-524, 1986.
- Suzana, P., Madhusudan, L., and Avram, B., "Bypass Effect in High Performance Heat Sinks," Submitted to the Int. Thermal Sciences Conference in Bled, Slovenia, June 11th-14th, 2000.
- Webb, R. I., and Gupte, H., "Design of Light Weight Heat Exchangers for Air to Two Phase Service," Compact Heat Exchangers, pp. 311-334., 1990, Hemisphere, New York.
- Wirtz, R. A., Chen, W., and Zhou, R., "Effect of Flow Bypass on the Performance of Longitudinal Fin Heat Sinks," ASME J. of Electronic Packaging, Vol. 116, pp.206-211, 1994.

- Zang, L.W., et al, "Heat Transfer Enhancement Mechanisms in Inline and Staggered Parallel Plate Fin Heat Exchangers," Int. J. of Heat and Mass Transfer, Vol.40, No.10, pp. 2307-2325, 1997.

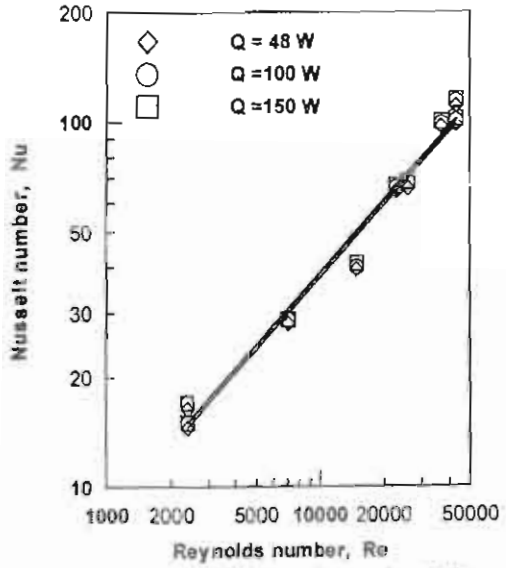

Fig. 4 Variation of Nusselt number with Reynolds number for straight fin array at different power input.

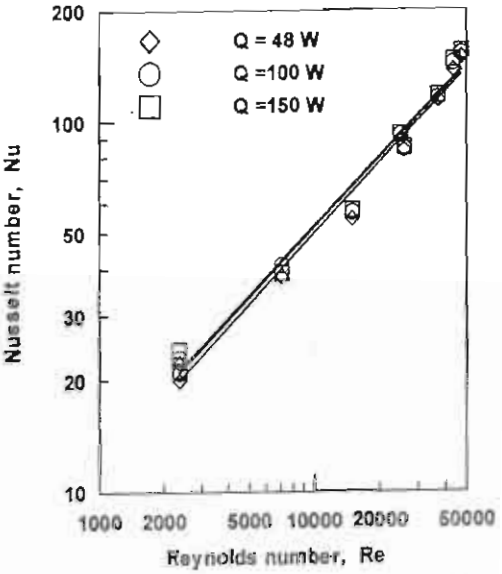

Fig. 5 Variation of Nusselt number with Reynolds number for corrugated fin array at different power input.

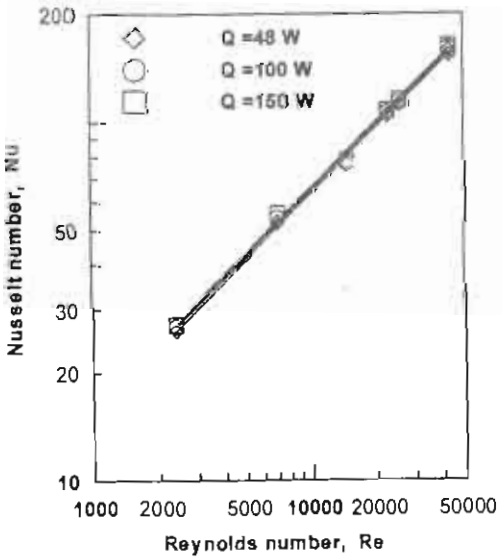

Fig. 6 Variation of Nusselt number with Reynolds number for mixed fin array at different power inp. .

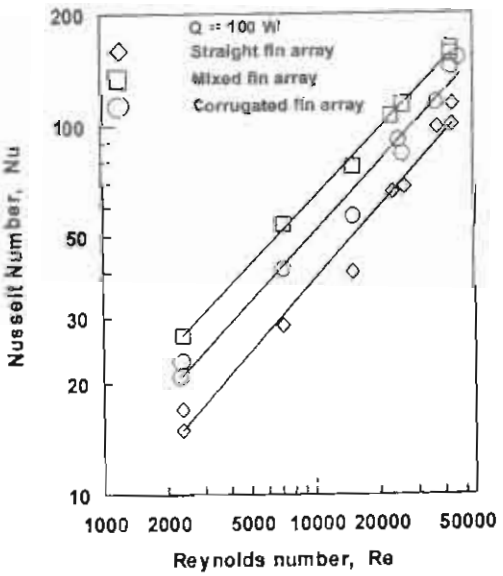

Fig. 7 Variation of Nusselt number with Reynolds number for the tested fin arrays at constant power input.

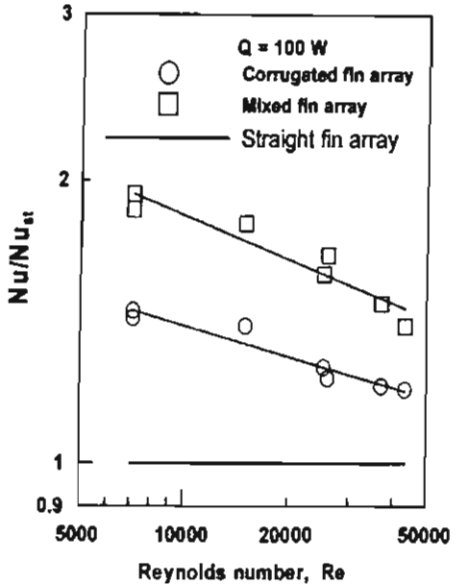

Fig. 8 Percentage enhancement in Nusselt number versus Reynolds number for the tested fin arrays at constant power input.

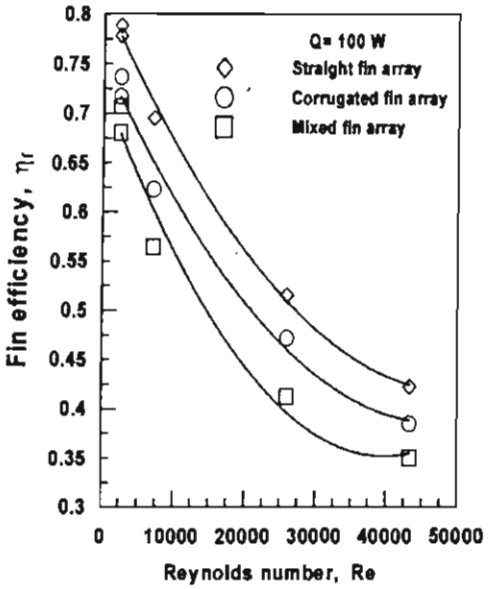

Fig. 9 Efficiencies of the tested fin arrays versus Reynolds number at constant power input.

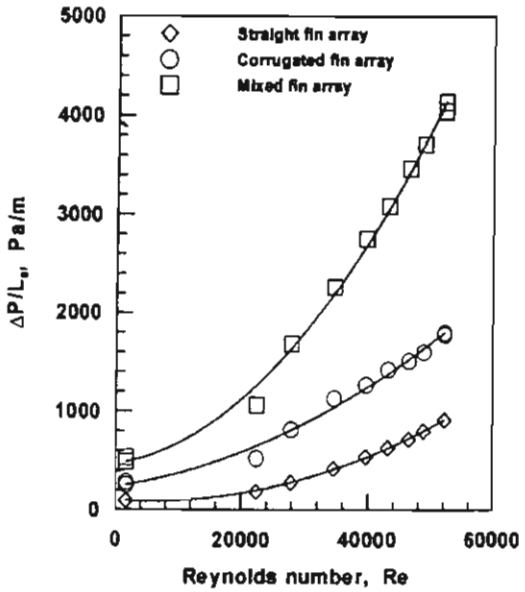

Fig. 10 Pressure drop variation with Reynolds number for the tested fin arrays.

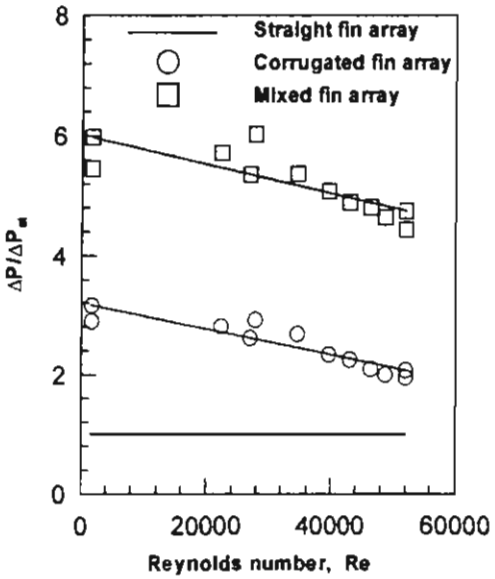

Fig. 11 Percentage increase in pressure drop against Reynolds number for the tested fin arrays.

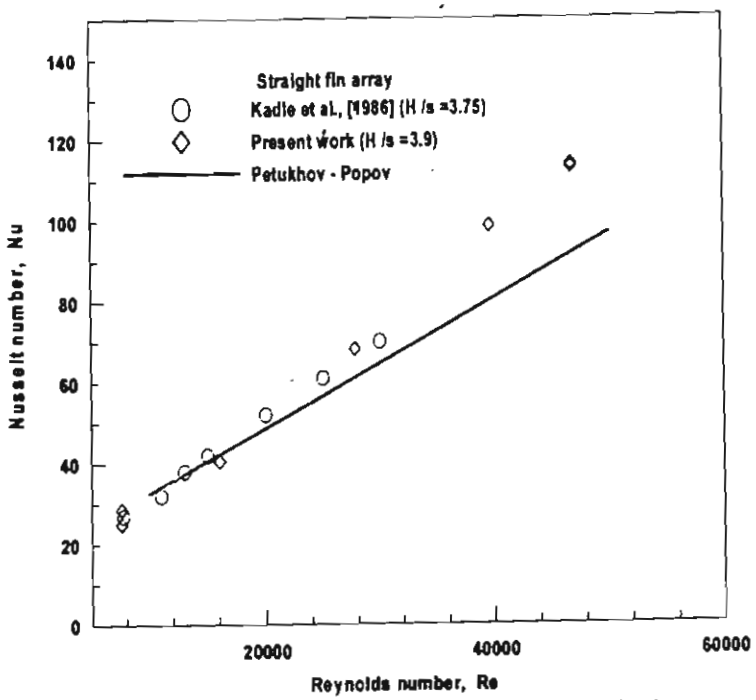

Fig. 12 Comparison of present experimental results with others.